Journal of King Saud University – Science 34 (2022) 102165

Contents lists available at ScienceDirect

Journal of King Saud University – Science

journal homepage: www.sciencedirect.com

Original article

The protective effect of isoliquiritigenin against doxorubicin-induced nephropathy in rats entails activation of Nrf2 signaling as one key mechanism

Wahidah H. Al-Qahtani [a], Ghedeir M. Alshammari [a,*], Mohammad A. Alshuniaber [a], Mureed Husain [b], Sarah A. Alawwad [a], Salwa T. Al-Ayesh [a], Mohammed Abdo Yahya [a], Abdulrahman S. Aldawood [b]

[a] Department of Food Science and Nutrition, College of Food and Agricultural Sciences, King Saud University, Riyadh, Saudi Arabia
[b] Economic Entomology Research Unit, Department of Plant Protection, College of Food and Agriculture Sciences, King Saud University, Riyadh, Saudi Arabia

ARTICLE INFO

Article history:
Received 24 April 2022
Revised 23 May 2022
Accepted 8 June 2022
Available online 14 June 2022

Keywords:
Isoliquiritigenin
Doxorubicin
Nrf2
Antioxidant
Kidney

ABSTRACT

Objectives: This study aimed to evaluate if the protective effect of Isoliquiritigenin (ISL) against doxorubicin-induced nephropathy in rats entails activation of Nrf2 signaling.
Methods: Adult male Wistart rats were treated as control, ISL, DOX, DOX, and ISL + DOX + ISL + Nrf2 inhibitor (brusatol) (n = 8/group). Treatments with ISL (25 mg//kg, oral) were carried out 10 days before and 10 days after the single dose of DOX (15 mg/kg, i.p).
Results: Treatment with ISL attenuated the glomerular and tubular damage and reduced interstitial fibrosis and collagen accumulation in the kidneys of DOX-intoxicated animals. It also increased urinary flow and volume, stimulated urinary creatinine excretion, and decreased albumin excretion. These effects were associated with high transcription of Bcl2, suppression of ROS, MDA, and inflammatory cytokines production (i.e., TNF-α, IL-6, and IL-1β), downregulation of apoptotic markers (Bax and caspase-3/9), TGF-β1, Collagen I/III. Besides, ISL stimulated renal expression, translation, and nuclear localization of Nrf2, as well as levels of GSH and SOD, independent of keap-1. All these effects afforded by ISL were reversed by suppressing Nrf2 with brusatol.
Conclusion: Pre-treatment with ISL is an effective strategy to alleviate DOX-induced nephropathy in rats by stimulating the Nrf2/antioxidant axis, which encourages further pre-clinical studies.

1. Introduction

Anticancer therapy has revealed Doxorubicin (DOX) as one of the active anticancer drugs that can treat solid and hematological cancers (Thorn et al., 2011). However, DOX therapy is associated with several adverse impacts on our health, including nephrotoxicity (Thorn et al., 2011). In this view, clinical and experimental studies have depicted early renal damage after a single and repetitive administration of dose DOX, an effect that involves overgeneration of reactive oxygen species (ROS) and inflammatory mediators, as well as scavenging the cell antioxidants (Soltani Hekmat et al.,2021; Savani et al., 2021). Despite this, literature still needs to determine the major oxidant molecular mechanisms underlying the nephrotoxic potential of this drug.

The redox-sensitive factor, the nuclear factor erythroid 2 related factor-2 (Nrf2), is the major cellular molecule that resists oxidative stress-mediated cell death (Hennig et al.,2018). Kepa-1 is a natural cytoplasmic inhibitory protein for Nrf2, which can sense ROS and electrophiles (Hennig et al.,2018). During non-stressful conditions, the transcriptional activity of Nrf2, which is constitutively synthesized, is limited as the newly synthesized Nrf2 molecules are captured by Keap-1 and are degraded through the ubiquitin–proteasome pathway (Hennig et al.,2018). However, ROS and elec-

Abbreviations: ISL, Isoliquiritigenin; DOX, Doxorubicin; ROS, Reactive oxygen species; Nrf2, Nuclear factor erythroid 2 related factor-2; ARE, Antioxidant response element; LPS, Lipopolysaccharides; CMC, Carboxymethylcellulose; Cr, Creatinine; TNF-α, Tumor necrosis factor-alpha; GSH, Total glutathione; SOD, Superoxide dismutase; MDA, Malondialdehyde.

* Corresponding author at: Riyadh, 11451, P.O. Box 2460, Saudi Arabia.
E-mail address: aghedeir@ksu.edu.sa (G.M. Alshammari).

Peer review under responsibility of King Saud University.

Production and hosting by Elsevier

https://doi.org/10.1016/j.jksus.2022.102165
1018-3647/

trophiles can phosphorylate specific cysteine residues on keap-1, thus facilitating the nuclear jumping of Nrf2 and binding to the antioxidant response element (ARE) to start the transcription process (Hennig et al.,2018; Serafini et al., 2020). In this regard, Nrf2 stimulates cell antioxidant defense systems by promoting the synthesis of glutathione (GSH) and phase II antioxidant enzymes such as NAD(P)H: quinone oxidoreductase 1 (NQO1), catalase, superoxide dismutase, and heme oxygenase-1 (HO-1) (Ganesh et al., 2013). Besides, Nrf2 inhibits cell inflammation and suppresses intrinsic (mitochondria-mediate) cell apoptosis by inhibiting NRLP3 inflammasome and NF-κB, as well as upregulating Bcl2 anti-apoptotic protein (Wardyn et al., 2015; Hennig et al.,2018). Interestingly, the expression and the transcriptional activities of Nrf2 are depleted in the majority of nephrotic disorders and are common upstream pathways underlying the associated oxidative/inflammatory damage (Guerrero-Hue et al., 2020). Likewise, DOX-induced renal, hepatic, and cardiac damage is committed by suppressing Nrf2 (Guo et al., 2018; Lin et al., 2018). However, these adverse effects of DOX prevented pharmacological activation of Nrf2 (Lin et al., 2018). Hence, searching for therapeutics from natural resources which can activate Nrf2 will provide novel pharmaceutical drugs that may reduce the burden of DOX use and open a new hope for continuing treatment with DOX.

The examination of the potential of the plant-derived flavonoids in the treatment of kidney disorders and alleviating DOX-induced toxicities have been under focus during the last years. The flavonoid, Isoliquiritigenin (ISL), obtained from the *Licorice* plant, is well-known for its pharmacological activities (Peng et al., 2015). Research, cross-sectional, and clinical studies have confirmed that treatment with ISL could alleviate cardiac, pulmonary, renal, and hepatic damage in various animal models by suppressing oxidative stress and inflammation (Peng et al., 2015). Indeed, ISL protected against triptolide, lipopolysaccharides (LPS), carbon tetrachloride (CCL4), *tert*-butyl hydroperoxide, and cadmium chloride (CdCl2)-induced liver damage in rodents by activating Nrf and parallel suppression of NF-κB (Zhao et al., 2015; Park et al., 2016; Cao et al., 2016; Chen et al., 2018). It also prevented experimentally induced Hepatic sinusoidal obstruction syndrome (HSOS) by activating Nrf2 signaling (Huang et al., 2018). With respect the kidneys, ISL also inhibited cisplatin, diabetic, and unilateral ureteral obstruction (UUO) as well as carrageenan-induced pleurisy by suppressing the generation of ROS, upregulation of antioxidants, suppressing NF-κB, and activating Nrf2 (Lee et al., 2008; Zhao et al., 2012; Liao et al., 2020; Gao et al., 2020; Alzahrani et al., 2021). ISL also attenuated angiotensin II (ANG II)-mediated hypertensive renal damage by activating Nrf2 (Xiong et al., 2018). In the same manner, ISL also alleviated hyperglycemia-induced renal damage in culture by upregulating and activating SIRT1 and Nrf2 (Huang et al., 2020).

Until now, the nephroprotective effect of ISL against DOX-induced renal damage, as well as the mechanisms of protection, was never shown before. Therefore, in this investigation, we have tested if pre-administration of ISL could prevent nephropathy in rats exposed to DOX and if this protection is triggered by activation/upregulation of Nrf2.

2. Materials and methods

2.1. Animals

Adult Wistar rats (14 weeks; 270 ± 15 g) were obtained from and kept in the Experimental Animal Care Center at King Saud University in Riyadh, KSA. The animals were always housed under ambient conditions of 21 ± 1℃, the humidity of 61 %, and the 12 h dark-light cycle. Through all weeks of the study, they also had free access to their diet and drinking water. The ethical approval was obtained from the institution's ethical committee before running the experiments (IRB No. KSU-SE-21–17).

2.2. Drugs

ISL (# HY-N0102) was purchased from Med Chem Express LLC (NJ, USA). Brusatol, a selective Nrf2 inhibitor (# SML1868), carboxymethylcellulose (CMC) (# C5013), and DOX hydrochloride solution (# D1515) were supplied by Sigma Aldrich (MO, USA). 0.5 % of CMC was used as a drug carrier (vehicle) for ISL and brusatol.

2.3. Experimental design

Animals were randomly classifed ito 5 groups (n = 8/group) as **1) control-group:** orally administered 0.5 % CMC for 20 days and daily; **2) ISL-treated-rats:** daily administered ISL dissolved in 0.5 % CMC at a final concentration of 25 mg/kg mg/kg for 20 days; (**3) DOX-model group:** injected (i.p.) with a single dose of DOX (15 mg/kg in normal saline) on day 10 and were orally and daily administered 0.5 % CMC,10 days before and after, treatment with DOX; **4) ILS + DOX-treated group:** injected (i.p.) with a single dose of DOX (15 mg/kg in normal saline) on day 10 and were orally and daily administered ISL (25 mg/kg),10 days before and after, treatment with DOX; **and 5) ISL + DOX + brusatol**: treated exactly as in the previous group but a concomitant i.p. injection of brusatol, dissolved in 0.5 % CMC (2 mg/kg), every 2 days for the 20 days of the study. Final body weights were measured by the end of the study whereas food intake was measured weekly.

2.4. Dose selection

A single dose of DOX at a dose of 15 mg/kg induced renal damage and nephropathy in rats 10 days post-treatment (Song et al.,2019). ISL at concertation of 25 mg/kg attenuated UUO-induced nephropathy in rats (Liao et al., 2020). Brusatol, at this tested concentration, was used in vivo by multiple authors to suppress Nrf2 in various organs of rats, including the kidneys (Shatoor et al., 2022).

2.5. The 24 h urine collection

On day 21, all rodents were housed in metabolic cages, and their urine was collected over 24 h. Urine volume was measured and preserved at −20℃ until use.

2.6. Blood and kidneys collection and processing

After urine collection, anesthesia was introduced to every rat by ketamine/Xylazine hydrochloride (80:10 mg/kg, i.p). Blood was collected by cardiac puncture and used to isolate the serum (1300 × g/10 min). Blood samples were preserved at −20℃ until analysis. Then each animal was authenticated, and its kidneys were isolated and cut into smaller sections of 4–5 mm. These sections were preserved at −80℃ or sent to the pathology lab for evaluation.

2.7. Assessment of kidney function

Assay kits were used to measure the concentration of the urea in the frozen serum (# DIUR-100 BioAssay Systems, CA, USA, and # EIABUN, ThermoFisher Scientific, Germany). An assay kit was used for the measurement of the creatinine (Cr) and albumin in the urine and blood (# MBS841754, MyBioSorces, CA, USA). Cr execration (per 24 h) and Cr clearance (CrCl) were determined using the equation described by Bazzano et al. (2015) using these formu-

las [(CrE (mg) = urinary Cr (mg/dl) × urine volume in 24 h) and (CrCl (ml/min) = urine creatinine (mg/dl) × urine flow (ml/min)/ serum creatinine (mg/dl)]. The urine flow (ml/min) was determined by dividing urine volume over 1440. All protocols were conducted per each kit's instructions, and the absorbance was read using a microplate reader (Model VERSAmax, Molecular Devices, USA).

2.8. Biochemical analysis in the kidneys

Frozen kidney tissue (70 mg) were homogenized in 0.5 ml ice-cold PBS (pH = 7.4) and supernatants were collected (12000 × *g*/4℃/20 min). All supernatants were frozen at −80℃ and used later to measure levels of some oxidative stress and inflammation-related markers. At the same time, the nuclear extracts were prepared from other kidney samples using a special kit (# Ab113474, Abcam, Cambridge, USA). A Cayman assay kit (# 10009055, USA) was used to assess the levels of malondialdehyde (MDA). ELISA was used to determine the renal levels of total glutathione (GSH) (# orb782371, Biorbit, MO, USA), superoxide dismutase (SOD) (# MBS036924,); tumor necrosis factor-alpha (TNF-α) (# BMS622, ThermoFisher), interleukine-6 (IL-6) (# R6000B, R&D System, MN, USA), and IL-1β (Ab100768, Abcam, Cambridge, USA). ELISA kits purchased from MyBioSource, CA, USA, were used to assess the nuclear and total homogenate levels of NF-κB p65 and Nrf2 (# MBS2505513 and # MBS752046). All protocols followed the suppliers' instructions using the VERSAmax microplate reader, Molecular Devices, USA).

2.9. Real-time PCR (qPCR)

All primers used for this part we purchased from ThermoFisher Scientific (Table 1). The Trizol (TRI) reagent (# T9424, Sigma Aldrich, MO, USA) was used to extract the RNA from each renal sample. iScript preparation kit (# 1708891, Bio-Rad, USA) was used to build the first-strand cDNA. Amplification was conducted in CFX 348 qPCR machine (BioRad, USA) (20 μl/well) using Evergreen Supermix (# 172–5200, BioRad, USA). With the following ingredients: master mix reagent (10 μl), forward primer (0.2 μl/500 nM), reverse primer (0.2 μl/500 nM); template cDNA (2 μl/50 ng), nuclease-free water (7.2 μl). qPCR steps were heating (1 cycle/98℃/30 *sec*), denaturation (40 cycles/98℃/5 *sec*), annealing (40 cycles/60℃/5 *sec*), and melting (1 cycles/95℃/5 *sec*/step). Normalization was performed against β-actin and the ΔΔCT method.

Table 1
Primers characteristics of the real-time PCR.

Gene	Primers (5′→3′)	GenBank accession #	Product length
Nrf2	F: - AAAATCATTAACCTCCCTGTTGAT R: R: ′- CGGCGACTTTATTCTTACCTCTC	NM_031789	118
Keap-1	5′-TATGAGCCAGAGCGGGACGA-3′ 5′-TCATCCGCCACTCATTCCTCT-3′	AF304364.1	172
Bcl2	F: TGGGATGCCTTTGTGGAACT R: TCTTCAGAGACTGCCAGGAGAAA	U34964.1	73
Bax	F: ATGGAGCTGCAGAGGATGATT R: TGAAGTTGCCATCAGCAAACA	NM_017059	97
Caspase-3	F: AATTCAAGGGACGGGTCATG R: R-GCTTGTGCGCGTACAGTTTC	U49930	67
Caspase-8	F: TGGTATATCCAGTCACTTTG R: CTCACATCATAGTTCACGCCAGTC	AF279308.1	95
Caspapse-9	F: AGCCAGATGCTGTCCCATAC R: CAGGAGACAAAACCTGGGAA	NM031632	55
Col 1A1	F: ACAGTCGATTCACCTACAGC R: TGTCCAAGGGAGCCACATCG	NM_053304	132
Col 3A1	F: CACTTACACAGTTCTAGAGG R: ATGTCATAGGGTGCGATATC	NM_032085	
Tgfb1	F: CCATGCCAACTTCTGTCTGGG R: GGCACGCAGCACGGTGATG	NM_021578.2	123
B-actin	F: ATC TGG CAC CAC ACC TTC R: AGC CAG GTC CAG ACG CA	NM_031144	291

2.10. Histopathological and electron microscope study

For the histology, kidney sections were first fixed in 10 buffered formalin for 16 h and then rehydrated in decreasing concentrations of alcohol, embedded in wax, cut (3–5 μ, and then routinely stained Harris hematoxylin (H) and Eosin (E). For the electron microscopy examination, kidney parts (0.05 mm^3) were kept in 3 % glutaraldehyde buffer (pH 7.4) for 6 h in a fridge, re-fixed using 1 % osmium tetroxide phosphate buffer (1 h). and dehydrated in ethanol. These samples were then embedded in Araldite risen, cut (1 μm), and stained with uranyl acetate and lead citrate. Histological sections were examined under the light microscopy, whereas those of the ultrastructures were examined using the transmission electron microscope (JEM-1011, JEOL Co., Tokyo, Japan).

2.11. Statistical analysis

All data were analyzed, and graphs were generated using the GraphPad Prism statistical software (Version 8, USA). Analysis was conducted using one-way ANOVA. The post hoc test was Tukey's test. Prior analysis normality of the data was confirmed using the Kolmogorov-Smirnov test. Data were considered statistically varied at $P < 0.05$ and were presented in the tables as means ± standard deviation (SD).

3. Results

3.1. ISL increases final body weights without changing food intake in DOX-treated rats

ISL-treated rats showed no significant variations in their final body weights, food intake, or any of the measured kidney markers as compared to control rats (Table 2). DOX-administered rats showed a significant reduction in body weights and food intake versus the control rats (Table 2). Also, food intake was not statistically changed when DOX, DOX + ISL, and DOX + ISL-brusatol-trea ted rats were compared with each other, indicating no significant effect of ISL or brusatol on body weights (Table 2). On the opposite, there was a significant increment in ISL + DOX-treated rats' body weights compared to DOX-treated rats (Table 2). This was significantly reversed in DOX + ISL + brusatol-treated rats (Table 2). No significant variation in food intake was observed between DOX + ISL + brusatol as compared to DOXmodel rats (Table 2). These data indicated the ISL-induced weight gain is an Nrf2-dependent mechanism.

3.2. ISL improves kidney function tests in DOX-treated rats

All measured markers of the kidney function were not statistically varied between the ISL-treated rats and control rats (Table 2). Compared to control, there are higher levels of serum urea and Cr and increased urinary albumin levels with a significant reduction in the urine volume, urine flow, urinary Cr, and CrCl in the DOX-intoxicated animals (Table 2). These animals also showed a high urinary albumin/Cr ratio (Table 2). An opposite biochemical picture

Table 2
Final body weights, food intake, and markers of kidney function in all groups of rats.

Parameter	Control	ISL	DOX	ISL + DOX	ISL + DOX + brusatol
Final body weights (g)	352.7 ± 17.5	349.7 ± 16.8	278.4 ± 13.4[ab]	331.5 ± 12.1[c]	328.7 ± 15.7[abcd]
Weekly food intake (g/group)	1435.4 ± 118.1	1501.3 ± 130.3	878.5 ± 110.1[ab]	938 ± 91.1[ab]	891 ± 84.3[ab]
Serum					
Albumin (g/dl)	6.81 ± 0.93	6.62 ± 0.89	3.14 ± 0.76[ab]	5.23 ± 1.1[bc]	3.04 ± 0.81[abd]
Urea (mg/dl)	4.56 ± 0.87	5.1 ± 0.91	56.1 ± 5.8[ab]	14.5 ± 2.6[abc]	61.4 ± 7.1[abd]
Creatinine (mg/dl)	0.65 ± 0.15	0.66 ± 0.12	3.41 ± 0.86[ab]	0.91 ± 0.24[abc]	3.67 ± 0.72[abd]
Urine					
Volume (ml/24 h)	15.1 ± 1.46	14.8 ± 1.65	9.3 ± 1.5[ab]	13.7 ± 1.7[c]	9.1 ± 1.1[abd]
Urine flow (μl/min)	10.5 ± 0.76	10.3 ± 1.14	6.5 ± 1.05[ab]	9.6 ± 0.99[c]	6.3 ± 0.83[abd]
Albumin (Alb) (μg/dl)	16.5 ± 3.4	17.8 ± 2.7	71.5 ± 7.9[ab]	26.8 ± 3.8[abc]	70.4 ± 11.4[abd]
Creatinine (mg/dl)	73.4 ± 6.2	70.4 ± 12.4	19.8 ± 4.4[ab]	61.8 ± 5.7[abc]	21 ± 6.3[abd]
Urinary Alb/Cr ratio (μg/mg)	0.23 ± 0.061	0.25 ± 0.053	3.6 ± 1.02[ab]	0.43 ± 0.13[abc]	3.3 ±.09[abd]
CrCl (ml/min)	0.86 ± 0.21	0.81 ± 0.16	0.036 ± 0.013[ab]	0.46 ± 0.06[abc]	0.034 ± 0.015[abd]

Data are given as mean ± SD (n = 6 animals/group). [a]: vs control rats; [b]: vs ISL-treated rats; [c]: vs DOX-treated rats, and [d]: vs ISL + DOX-treated rats.

of all these markers was observed in ISL + DOX-treated rats versus DOX-treated rats. All these effects were reversed by Nrf2 inhibition (DOX + ISL + brusatol) as compared to ISL + DOX-treated rats (Table 2). Interestingly, similar non-significant levels of urine volume, urine flow, serum urea, and Cr, urinary albumin and Cr, and CrCl were seen when DOX-model rats were compared with DOX + ISL + brusatol-treated rats (Table 2). These data indicated that ISL's improvement in kidney function in DOX-treated rats is an Nrf2-dependent process.

3.3. ISL attenuates renal oxidative stress and inflammation in DOX-treated rats

A significant increase in the levels of GSH and SOD with a concomitant reduction in the levels of ROS and MDA, as well as mRNA, cytoplasmic, and nuclear levels of NF-κB were seen in the kidneys of ISL-treated rats as compared to control rats (Fig. 1**A-D and** Fig. 2**-A-F**). Levels of GSH and SOD were significantly decreased, but levels of ROS, MDA, IL-6, TNF-α, and IL-1β, as well as mRNA, cytoplasmic, and nuclear levels of NF-κB, were significantly increased in the kidneys of DOX-treated rats as compared to control rats (Fig. 1**A-D and** Fig. 2**A-F**). The levels of all these markers were significantly reversed in the kidneys of ISL + DOX-treated rats as compared to DOX-treated rats (Fig. 1**A-D and** Fig. 2**A-F**). No significant differences in the levels of all these markers were seen between DOX and DOX + ISL + brusatol. These data indicate that ISL attenuates renal oxidative stress and inflammation by scavenging ROS, inhibiting lipid peroxidation, upregulating antioxidants, and suppressing NF-κB and the generation of inflammatory cytokines through activating Nrf2.

3.4. ISL suppresses intrinsic cell apoptosis in the kidneys of DOX-treated rats

No significant alteration in the mRNA levels of Bax, Bcl2, caspase-3, and caspase-9 were seen between the control and ISL-treated rats (Fig. 3**A-D**). mRNA levels of Bax, caspase-3, and caspase-9 were significantly upregulated. However, mRNA levels of Bcl2 were significantly depleted in the kidneys of DOX-treated rats as compared to control rats. However, they have then reversed in the kidneys of ISL + DOX-treated rats as compared to DOX-treated rats (Fig. 3**A-D**). Administration of brusatol to ISL + DOX-treated rats significantly increased mRNA levels of Bax, caspase-3, and caspase-9. It lowered Bcl2 as compared to ISL + DOX-treated rats (Fig. 3**A-D**). These data suggest that the inhibitory effect of ISL on DOX-induced mitochondria-mediated (intrinsic) cell death requires activation of Nrf2 signaling.

3.5. ISL stimulates renal Nrf2 activation in DOX-treated rats

A significant increment in the total levels of Keap-1 with a significant reduction in the mRNA, cytoplasm, and nuclear levels of Nrf2 were observed in the renal tissues obtained from DOX-treated rats as compared to control rats (Fig. 4**A-D**). Levels of Keap1 were not significant, but mRNA, cytoplasm, and nuclear levels of Nrf2 were significantly higher in kidneys of ISL and ISL + DOX as compared to vehicle-treated control or DOX-model rats, respectively (Fig. 4**A-D**). However, ISL + DOX + brusatol-treated rats showed a significant reduction in the cytoplasmic and nuclear levels of Nrf2 as compared to ISL + DOX –treated rats (Fig. 4**A-D**). Interestingly, mRNA levels of Keap-1 and Nrf2 were not statistically varied in this group of rats as compared to ISL + DOX-treated animals (Fig. 4A-D). In addition, the reduction in the cytoplasmic and nuclear levels of Nrf2 in ISL + DOX + brusatol-treated rats were the maximum among all groups (Fig. 4**A-D**). These data suggest that ISL triggers the renal activation of Nrf2 activation by stimulating its transcription, translation, and nuclear translocation without modulating the expression of Keap-1 nor the degradation of Nrf2.

3.6. ISL improves the morphology of the kidneys in DOX-treated rats

Normal histological features, including normal glomeruli, Bowman's capsules, and renal and distal proximal convoluted tubules (DCT and PCT, respectively) were depicted in the control and ISL-treated rats (Fig. 5**A&B**). Sever tubular damage in the RCT and DCT with increased vacuolization and pyknotic nuclei, as well as moderate glomerular damage was seen in the kidneys of DOX-treated rats (Fig. 5**C**). On the contrary, almost normal glomerular and tubular features with few damaged tubules were seen in DOX + ISL-treated rats (Fig. 5**D**). Similar pathological changes like those seen in DOX-model rats were also observed in DOX + ISL + brusatol-treated rats (Fig. 5**E**).

3.7. ISL inhibits the transcription of TGF-β 1 and collagen transcription and deposition in the kidneys in DOX-treated rats

Very few collagen fibers were detected in the kidneys of both the control and ISL-treated animals (Fig. 6**IA&B and** Fig. 6**IIA**). Also, non-statistically varied but similar mRNA levels of TGF-β1, COL1A1, and COL3A1 were depicted in the control versus ISL-treated rats (Fig. 6**IIb&C**). On the opposite, increased collagen deposition with high mRNA levels of all above-mentioned genes was observed in the kidneys of DOX-treated rats, which were all significantly reduced again in the kidneys of ISL + DOX-treated rats

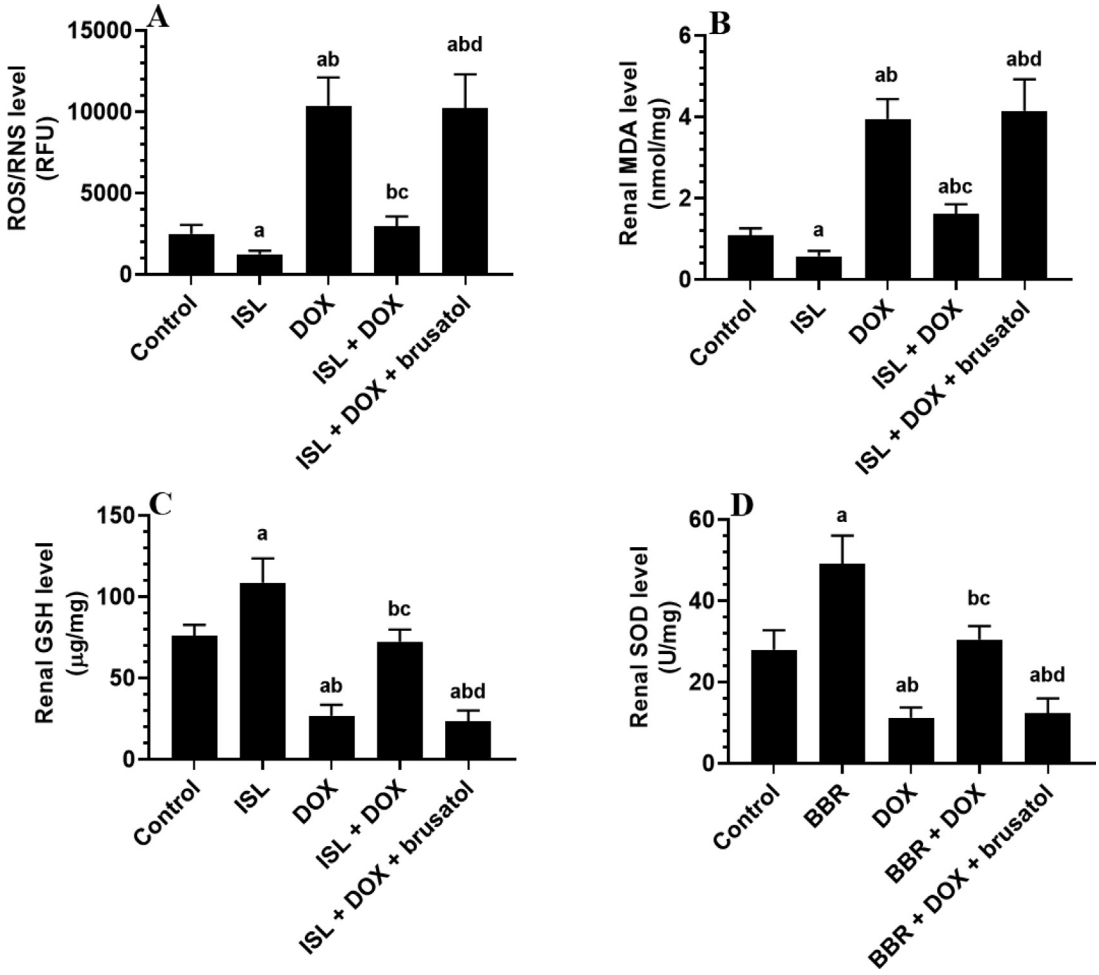

Fig. 1. The effect of DOX and ISL on the renal markers of oxidative stress of all experimental groups. Data are given as mean ± SD (n = 6 animals/group). [a]: vs control rats; [b]: vs ISL-treated rats; [c]: vs DOX-treated rats, and [d]: vs ISL + DOX-treated rats.

as compared to control rats (Fig. 6**IC&D,** Fig. 6**IIA-C**). On the other hand, the mRNA levels of TGF-β1, COL1A1, and COL3A1, as well as the amount of deposited were significantly increased in ISL + DO X + brusatol-treated rats as compared to ISL + DOX-treated rats but were not significantly varied as compared to DOX model rats (Fig. 6**IF,** Fig. 6**IIA-C**). These data indicate that ISL attenuated renal fibrosis and the TGFβ1 pathway by improving Nrf2 levels.

3.8. ISL improves the ultrastructural features in DOX-treated rats

Ultrastructural images obtained from the proximal renal tubules of the control rats that received the vehicle or ISL showed normal epithelial cells lying on an intact basement membrane with normal mitochondria, nuclei, and folding membranes, as well as long microvilli (brush borders) (Fig. 7**A&B**). On the other hand, an increased number of necrotic epithelial cells with an increased number of swollen and damaged mitochondria and folding embraces and pyknotic nuclei were depicted in renal tissues of DOX-treated rats. The images obtained from this group of rats also showed increased collagen fibers in the interstitial area between epithelial cells (Fig. 7**C&D**). Almost normal epithelial cells containing normal mitochondria and intact nuclei, as well as long brush borders, were seen in the renal sample obtained from ISL + DOX-treated rats (Fig. 7**E**). **F:** Similar ultrastructural changes like those in DOX-treated rats were also seen in ISL + DOX + brusatol-treated rats (Fig. 7**F**). Scale bars, 2 µm.

4. Discussion

ISL is a common flavonoid that is widely used as a therapeutic agent against cancer, as well as cardiac, pulmonary, renal, and pulmonary disorders (Peng et al.,2015). The protective potential of ISL against renal damage is documented in several animal models and was explained by its ability to suppress oxidative stress and inflammation (Xiong et al., 2018; Liao et al., 2020). No previous studies have examined the potential nephroprotective effect of ISL in DOX-treated animals or humans. In accordance, this study revealed that early and daily administration of a previously reported therapeutic dose of ISL (25 mg/kg) could alleviate DOX-induced renal damage by inhibiting renal oxidative stress, inflammation, fibrosis, and apoptosis. In addition, activation of Nrf2 by ISL underlie is its main protective mechanism which seems independent of Keap-1 expression.

Adriamycin (DOX) is the most common animal model to induce chronic kidney disease (CKD) in rodents that represent similar features seen in humans with CKDs, including focal segmental glomerulosclerosis, podocyte injury, tubular damage and atrophy, inflammation, interstitial fibrosis (Soltani Hekmat et al.,2021; Montoya et al., 2013). Clinical laboratory findings were seen in DOX-treated animals or cancer patients, including albuminuria, reduced GFR, and reduced Cr clearance (Montoya et al., 2013). Besides, intoxication with DOX is associated with a reduction in body weight which was attributed to inhibition of appetite

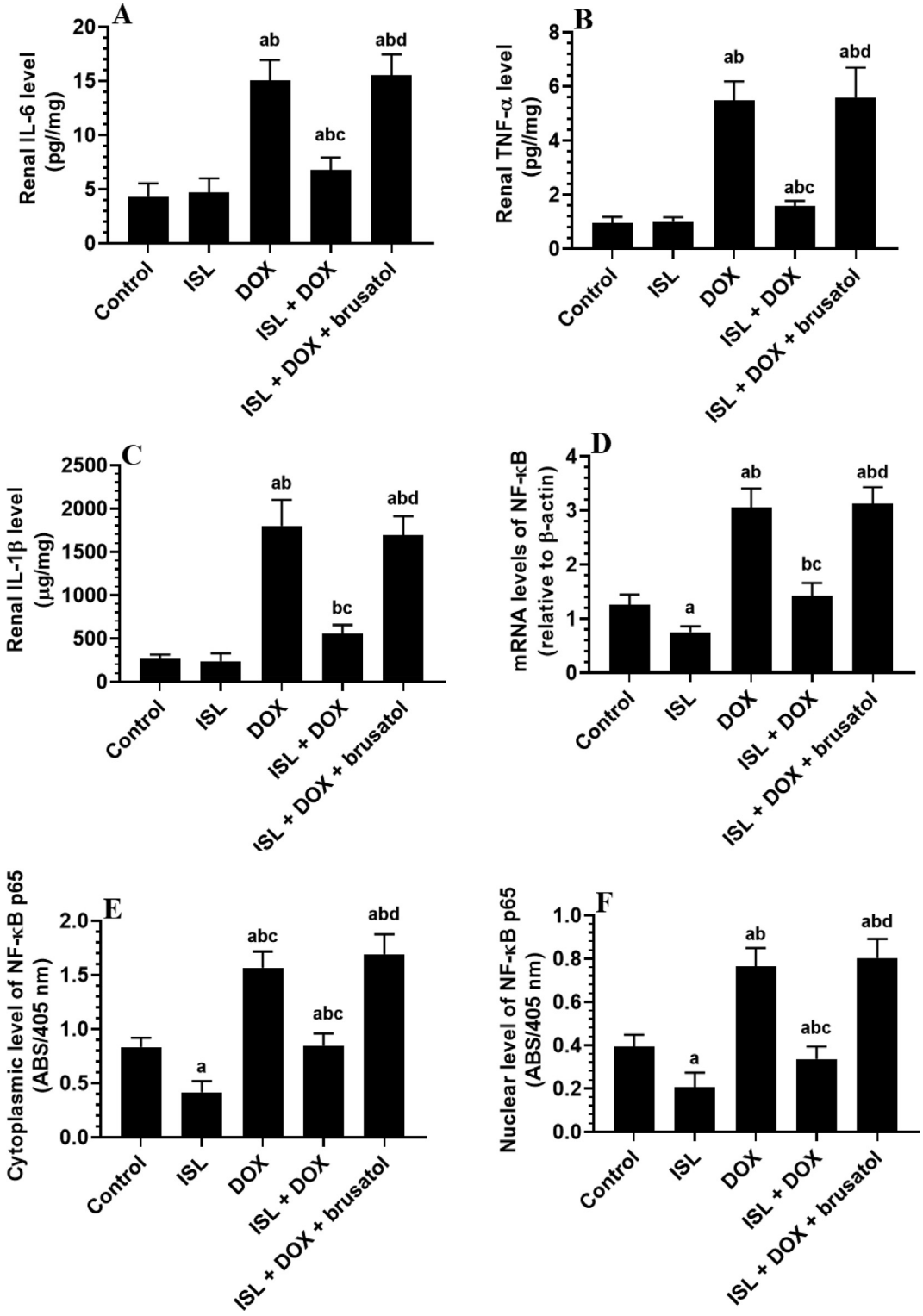

Fig. 2. The effect of ISL and DOX on renal levels of the inflammation-related markers of all experimental groups. Data are given as mean ± SD (n = 6 animals/group). [a]: vs control rats; [b]: vs ISL-treated rats; [c]: vs DOX-treated rats, and [d]: vs ISL + DOX-treated rats. MDA: malondialdehyde; SOD: superoxide dismutase; GSH: total glutathione; and ROS: reactive oxygen species.

(anorexia), suppression of adipose tissue lipogenesis and increased lipolysis, loss of skeletal muscle mass, and promotion of multi-organ organ damage (Canepari et al., 1994; Biondo et al., 2016). In rats, a single high dose of DOX or accumulative equivalent dose is sufficient to induce renal damage and nephropathy and results in all the above-mentioned pathogenesis. This has also been observed in DOX-treated rats of this current investigation, which validates this model and made suitable for studying the therapeutic potential of ISL. Accordingly, our data also report a potent nephroprotective effect of ISL against DOX-induced renal injury and dysfunction. This supports our initial hypothesis, which was based on previous studies which have also shown the ability of ISL to improve kidney

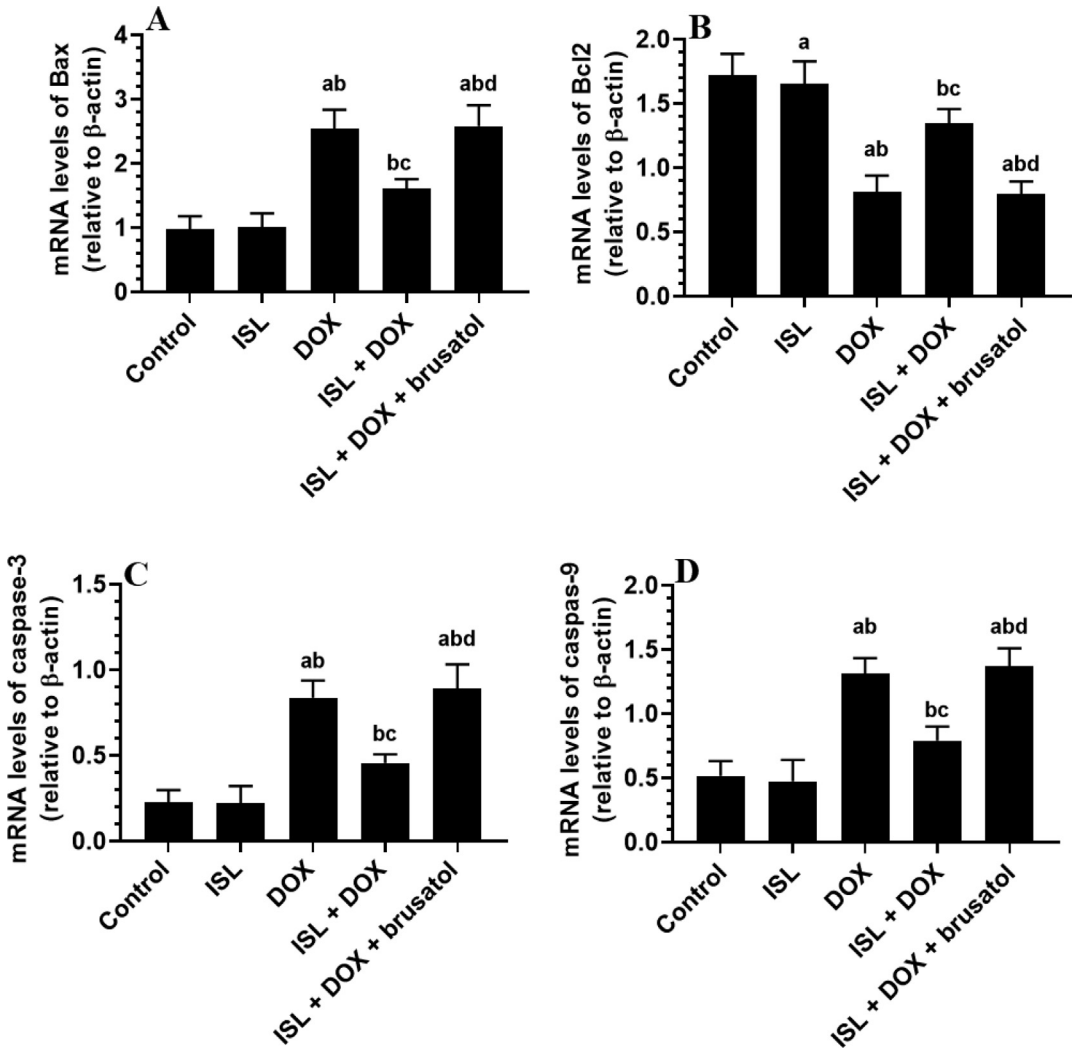

Fig. 3. The effect of ISL and DOX on renal mRNA levels of apoptotic/antiapoptotic markers of all experimental groups mRNA of some apoptotic and anti-apoptotic markers in the kidneys of all groups of rats. Data are given as mean ± SD (n = 6 animals/group). [a]: vs control rats; [b]: vs ISL-treated rats; [c]: vs DOX-treated rats, and [d]: vs ISL + DOX-treated rats.

tubular and glomerular structures, as well as markers of renal function and injury in other animal models, including those induced by hyperglycemia, diabetes, unilateral ureteral obstruction (UUO), ischemia, hypertension, and cisplatin (Xiong et al.,2018; Liao et al., 2020; Sun et al.,2021).

However, although administration of ISL didn't significantly improve food intake in the vehicle-treated or DOX-treated animals, the apparent increase in the bodyweight of in DOX-treated rats after administration of ISL could be explained by its ability to inhibit adipose tissue lipolysis and possibly through activating Nrf2. This can be confirmed as the administration of brusatol significantly prevented the improving effect of ISL on DOX-treated rat weights. Indeed, some studies have demonstrated the ability of Nrf2 to suppress lipolysis and stimulate adipogenesis in the adipose tissue (Sun et al., 2021).

The major triggers and hallmarks of the renal damage induced by DOX are oxidative stress and inflammation (Asaad et al., 2021). During DOX-intoxication, higher levels of ROS are generated in the kidneys and other tissue due to the upregulation of numerous ROS-generating enzymes [i.e. nitric oxide synthase (NOS), NADPH reductase, and Quinone dehydrogenase 1 (NQO1)], induction of Fe + 2-DOX adducts, and mitochondria damage, diminishing intracellular glutathione (GSH), and downregulation of enzymatic antioxidants (i.e. SOD, HO-1, and catalase) (Zhang et al., 2019; Asaad et al., 2021). Besides, DOX-induced nephrotoxicity is the activation of the inflammatory transcription factor NF-κB which promotes inflammation and oxidative stress by stimulating the synthesis/release of several adhesive molecules and inflammatory cytokines (Asaad et al., 2021). The activation of NF-kB and subsequent inflammation and oxidative stress responses are involved in a variety of renal disorders (Sanz et al., 2010). Of note, ROS and NF-κB can positively affect each other in a vicious positive feedback cycle (Wu et al., 2014).

The data from this study also support previous findings and suggest that DOX-mediated renal injury is caused by oxidative stress and inflammation. However, treatment with ISL significantly reduced ROS and MDA generation, attenuated the reduction in GSH SOD levels, and reduced the production of TNF-α and IL-6, as well as the nuclear activation of NF-κB p65 in the renal tissues of DOX model rats. In addition, ISL also improved levels of GSH and SOD and reduced the activation of NF-κB p65 in the renal tissues obtained from the control rats, thus confirming its potent antioxidant and anti-inflammatory properties under basal conditions. However, although not defiantly clear yet, it seems that the inhibitory effect of ISL on NF-κB in the kidneys of the rats of this investigation is secondary to its antioxidant effect. Indeed, the use of

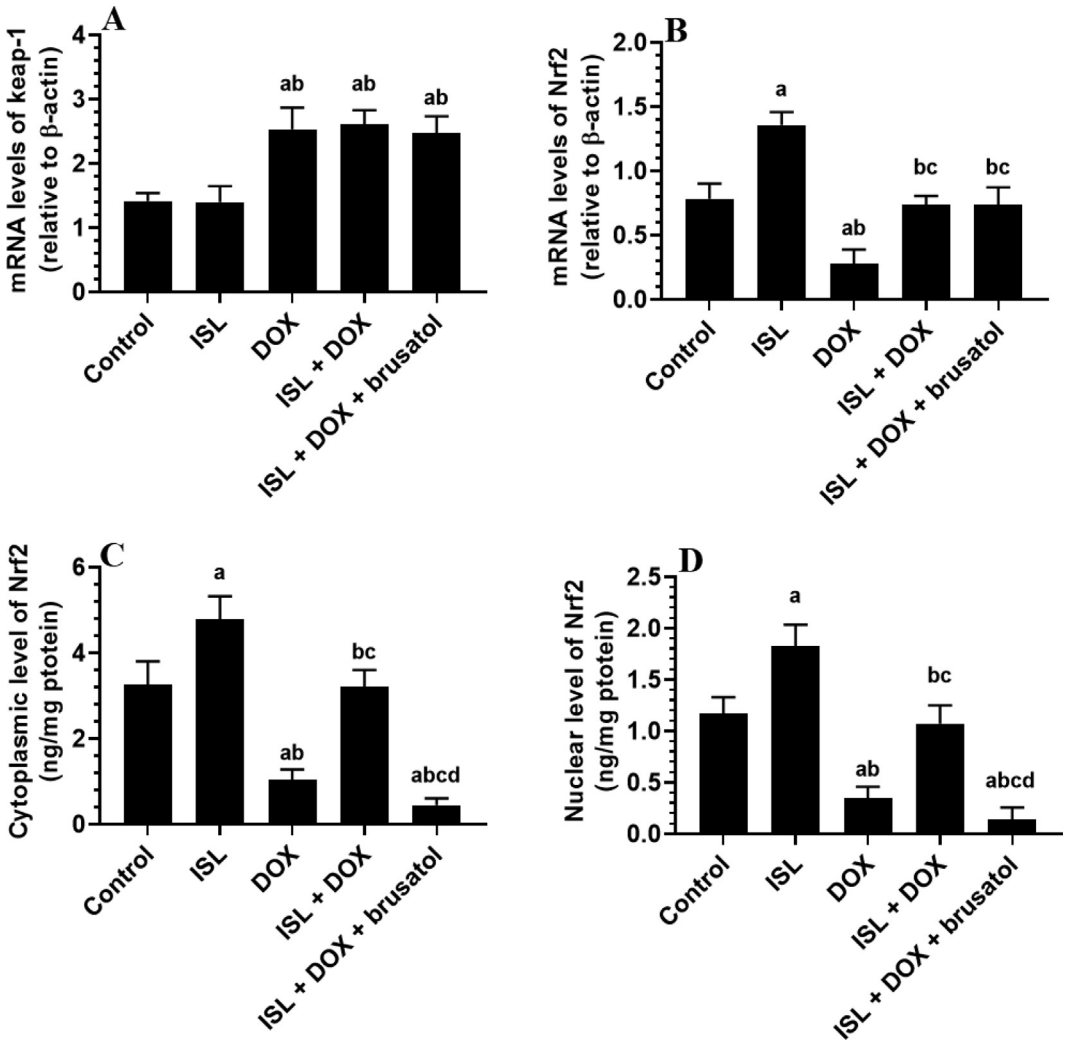

Fig. 4. The effect of DOX and ISL on renal Nrf2/keap1 pathway of all experimental groups. Data are given as mean ± SD (n = 6 animals/group). [a]: vs control rats; [b]: vs ISL-treated rats; [c]: vs DOX-treated rats, and [d]: vs ISL + DOX-treated rats.

antioxidants therapy (i.e., flavonoids and others) to treat DOX-induced renal and cardiac damage has shown that ROS act upstream and are major triggers for DOX-induced activation of NF-κB (Wu et al., 2014). Besides, ISL repressed the macrophage NF-κB p65 after exposure to LPS by direct upregulation of some antioxidant enzymes and independent of modulating Nrf2 (Wang et al., 2015).

Our findings support the study of sun et al. (Sun et al.,2021), who have previously demonstrated the ability of ISL to reduce ROS and stimulate GSH, SOD, and glutathione peroxidase-1 (GPX1) in the renal tissues of both the control and diabetic rats. The protective effect of ISL against cisplatin-mediated renal and hepatic damage was attributed mainly to its ability to upregulate GSH (Lee et al., 2008). Also, ISL reduced glutamate and 6-hydroxydopamine-mediated neural damage by suppressing ROS generation and upregulation of antioxidants (HWANG and CHUN, 2012). Furthermore, ISL prevented diabetic retinopathy and carrageenan-induced pleurisy in rats by upregulating GSH, SOD, and CAT, and repressing NF-κB (Gao et al., 2020; Alzahrani et al., 2021). In the same manner, ISL prevented UOO-induced renal damage by suppressing NF-κB and downregulating IL-1β, IL-6, and TNF-α (Liao et al., 2020).

On the other hand, renal fibrosis and apoptosis are key events mediating end-stage renal failure (ESRF) in various CKDs, including those induced by DOX (Ren et al., 2016). In general, renal fibrosis is induced by the over-activation of fibroblast due to a death signal and results in increased synthesis and deposition of extracellular matrix (ECM) protein such as collagen (Ren et al., 2016). TGF-β1 is the key player in this process, which can also promote the infiltration of inflammatory cells to initiate inflammation (Ren et al., 2016). High levels of TGF-β are linked to glomerulosclerosis, tubulointerstitial fibrosis, and epithelial-mesenchymal transition in various renal disorders and were also observed in the renal tissues of animals after exposure to DOX (Ren et al., 2016; Savani et al., 2021). Nevertheless, intrinsic (mitochondria-mediated) cell apoptosis is the major cell death modality observed in the renal cell after exposure to toxic doses of DOX (Lahoti et al., 2012). During intrinsic cell death, the imbalance in the expression of the apoptotic proteins (i.e., bax) versus the anti-apoptotic proteins (i.e., Bcl2) stimulates the translocation of the upregulated Bax to the mitochondria (Biondo et al., 2016). This leads to the damage to the mitochondria membrane, which results in releasing of the cytochrome-c and subsequent activation of a bunch of caspases (i.e., caspases-9/3).

The findings of this study also demonstrate a potent ability of ISL to suppress renal fibrosis and apoptosis in the renal tissues of DOX rats by attenuating mRNA levels of TGF-β, COL1A1, and COL3A1, caspase-3, and caspase-9. In addition, the anti-fibrotic

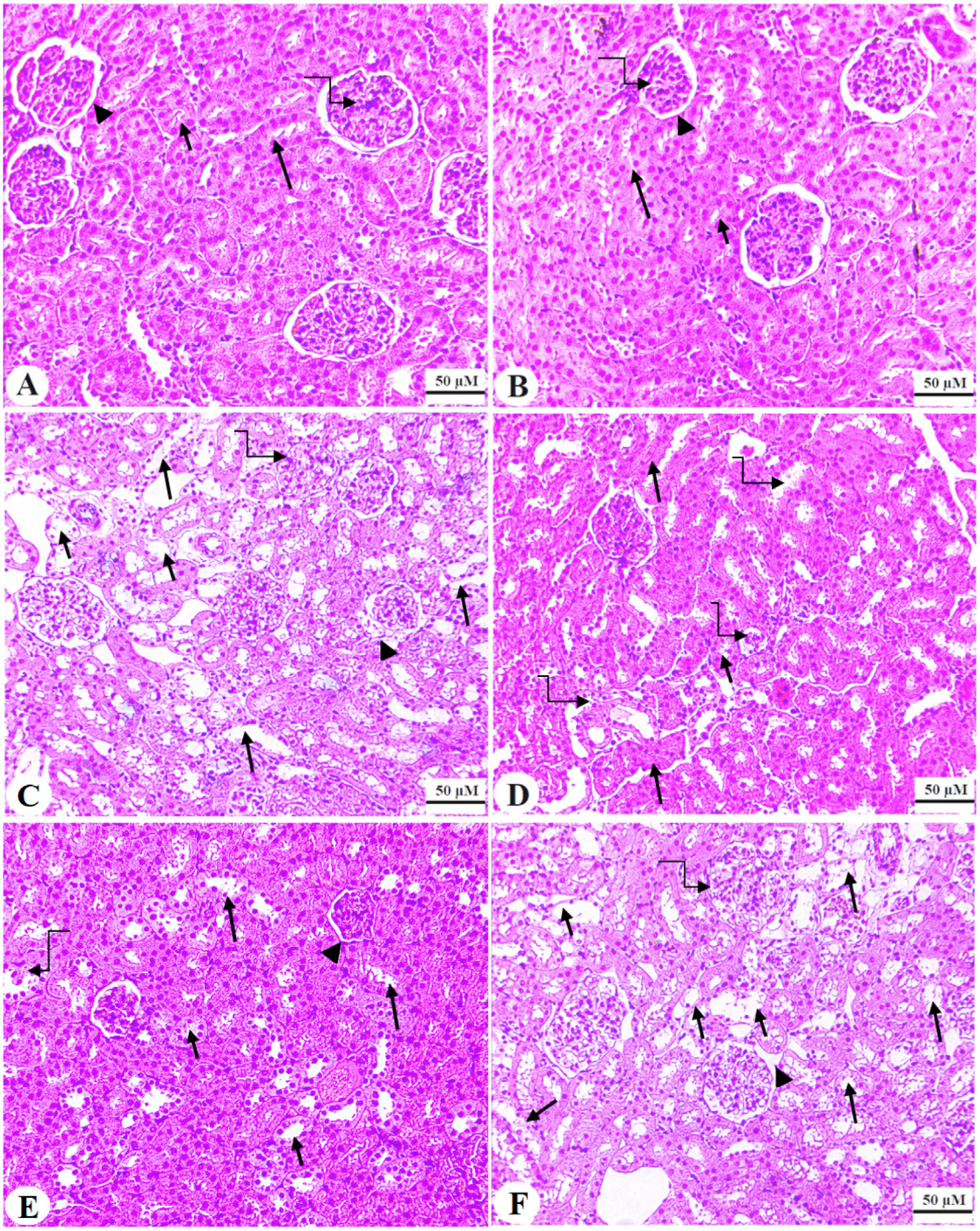

Fig. 5. Haematoxylin and eosin (H&E) sections obtained for the renal tissues of all groups. A and B: were taken from control and ISL-treated rats and showed normal glomerulus mass (curved arrow) and glomerular membrane (arrowhead). In addition, both the proximal and distal tubules convoluted tubules (PCT & DCT) appeared normal and intact (short and long arrow, respectively). C: represents a DOX model rat and showed damaged glomerular membranes (arrowhead), loss of Bowman's capsule space (curved arrow), and increased degeneration in both the PCT and DCT (short and long arrow, respectively). Note that increased number of tubular nuclei (curved arrow). D and E: represents ISL + DOX-treated rats and depict an obvious improvement in the structure of the glomerulus (arrowhead) and tubules (short and long arrow, respectively). However, degeneration in some PCT and DCT were also still seen (short and long curved arrows. F: represents an ISL + DOX + brusatol-treated animal and showed similar pathological changes like those observed in group C. 200x.

potential of ISL was also observed at the histological levels by the obvious attenuation of collagen deposition and tubular degeneration in the kidneys of DOX-treated animals. Since ISL does not affect the expression of all these genes in the kidneys of control rats, such fibrotic and anti-apoptotic potentials of ISL could be explained to be secondary to the reduction in ROS TNF-α production. Indeed, it has been demonstrated that ROS and inflammatory cytokines induced by DOX are the main triggers that activate renal fibrosis and apoptotic in the kidneys of rodents after exposure to DOX (Lahoti et al., 2012; Owumi et al.,2021). In this regard, several studies have shown that ROS can directly induce renal fibrosis by upregulating TGF-β1 (Montorfano et al.,2014; Ren et al., 2016). Likewise, TNF-α, and through the AP-1 pathway, can directly upregulate TGF-β1 (Sullivan et al., 2009). Also, ROS mediates

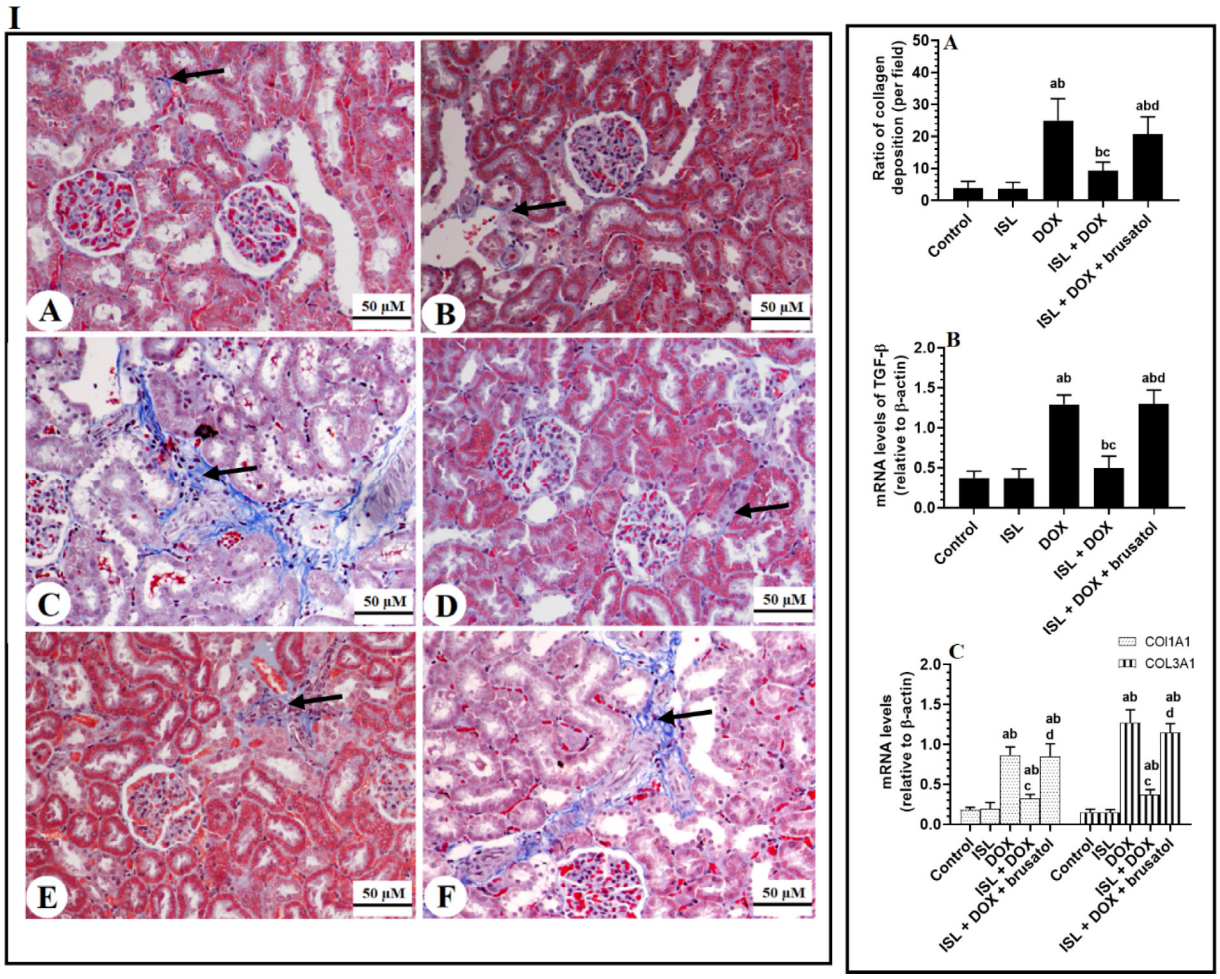

Fig. 6. Panel I: Masson Trichrome staining section for collage deposition (blue color) in the renal tissue of all groups of animals. Panel II: the number of collagen fibers deposited in the renal tissues as analyzed from panel A, as well as mRNA levels of TGF-β1, collagen 1A1 (COL1A1), and collagen 3A1 in the renal tissues of all groups of rats. Data are given as mean ± SD (n = 8 animals/group). [a]: vs control rats; [b]: vs ISL-treated rats; [c]: vs DOX-treated rats, and [d]: vs ISL + DOX-treated rats. 200X.

DOX-induced renal cell apoptosis by activating p53-dependent and independent apoptosis and by direct upregulation of apoptosis protein Bax and downregulating the anti-apoptotic protein, Bcl2 (Lahoti et al., 2012). Furthermore, TNF-α may directly induce intrinsic cell apoptotic by activating the caspase-8/Bid pathway (Zhao et al., 2003). Supporting our data, ISL attenuated renal fibrosis and apoptosis in diabetic and UUO-induced rats by suppressing ROS and inflammatory cytokines production (Sun et al., 2020).

On the other hand, the exact molecular mechanism behind the antioxidant and anti-inflammatory effect of ISL remained a challenging question for us. Hence, we have focused on the effect of ISL on Nrf2 given the importance of this pathway as an antioxidant and anti-inflammatory pathway (Ganesh et al., 2013; Wardyn et al., 2015). In addition, accumulating lines of evidence have confirmed that renal damage, fibrosis, and apoptosis induced by DOX are characterized by reduced activation of Nrf2, which can be prevented by Nrf2 activators (Lin et al., 2018; Elsherbiny and El-Sherbiny, 2014). Furthermore, ISL attenuated renal, cardiac, and hepatic injuries by activating Nrf2-mediating upregulation of antioxidants and repression of NF-κB p65 (Liu et al., 2017; Xiong et al., 2018; Zhang et al., 2018).

Supporting our evidence, an increment in the levels of Keap-1 with a parallel reduction in the transcription, translation, and nuclear localization of Nrf2 were observed in the renal samples obtained from DOX-treated animals. Similar to these data, the inhibitory effect of DOX on Nrf2 in the kidneys and other tissues activation was mediated by reducing the transcription and decreasing the degradation by upregulating Keap-1 (Lin et al., 2018; Nordgren and Wallace,2020). Opposing this, treatment with ISL stimulated the transaction of Nrf2 and enhanced its cytoplasmic and nuclear levels not only in the renal samples of DOX-intoxicated animals but also in the kidneys of the control rats, too. Interestingly, these events occurred with no significant alteration in the expression of Keap-1 in the renal samples obtained from both treated groups, thus dissipating the role of keap1 expression from the stimulatory effect of ISL on Nrf2. Such an increase in the activation of Nrf2 in the renal tissues of control and DOX-treated rats explains why they showed low levels of ROS, reduced activation of NF-κB, fewer levels of inflammatory cytokines, and higher levels of GSH, SOD, and CAT. To confirm it, we inhibited Nf2, in vivo, with a predetermined dose of brusatol. Brusatol can suppress Nrf2 nuclear translocation without altering the expression or levels of Keap-1 (Olayanju et al., 2015). Indeed, treatment with brusatol significantly depleted total and nuclear levels of Nrf2 without affecting mRNA levels of Nrf2 or Keap-1 in the renal samples of DOX + ISL-treated rats. In addition, treatment with brusatol abolished all the observed neuroprotection afforded by ISL and its previously discussed effect on ROS, antioxidants, NF-κB, and fibrotic and apoptotic markers. Based on this, ISL protection was based on activating Nrf2.

However, further mechanisms by which ISL could stimulate Nrf2 were not tested in this study which is considered one limita-

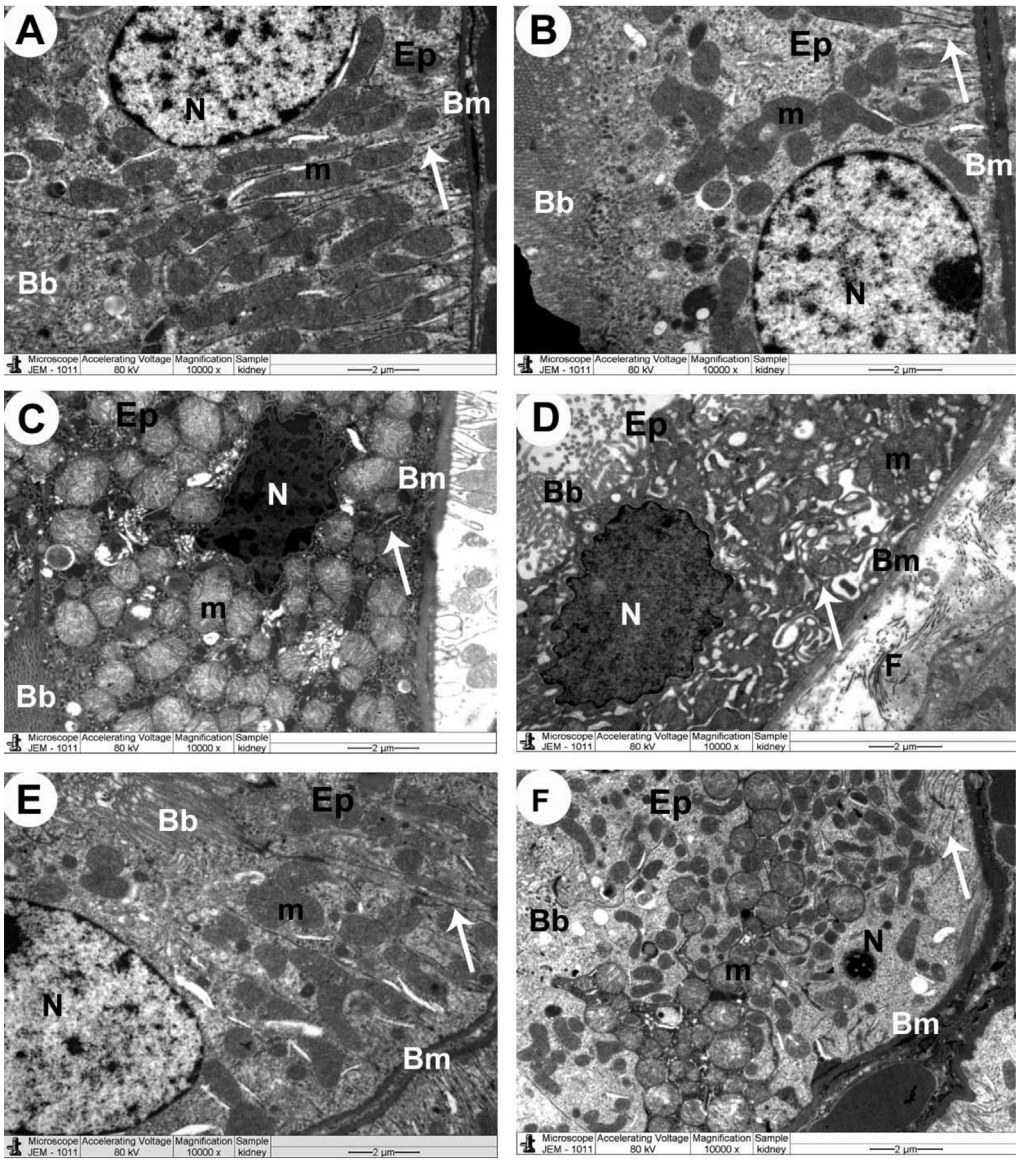

Fig. 7. Transmission electron micrographs (TEM) of the renal tubules obtained from all experimental groups A&B: Control and control + ISL-treated rats, respectively, and showed normal epithelial cells (Ep), round nucleus (N), mitochondria (m), basement membrane (Bm), infolding membranes (arrow), and brush border (Bb). C: A DOX-treated rat and demonstrated necrotic epithelial cell (Ep), which showed pleomorphic swollen and damaged mitochondria (m) and irregular-shaped pyknotic nucleus (N). Damaged infolding membranes (arrow) and brush border (Bb), as well as basement membrane (Bm), were also seen. D: a DOX-treated rat showed increased collagen fibers (F) in the interstitial area between epithelial cells. Apoptotic epithelial cell (Ep) shows damaged mitochondria (m) and irregular-shaped pyknotic nucleus (N). Pleomorphic damaged infolding membranes (arrow) and brush border (Bb), as well as basement membrane (Bm), were also seen. E: a DOX + ISL-treated rat showed improvement in the structure of the majority of the organelles forming the renal tubular cells F: a DOX + ISL + brusatol rat showing similar ultrastructural changes seen in the renal in C. Scale bar = 2 µm. 10000X.

tion in this study. However, previous studies have shown that ISL could stimulate Nrf2 in the hepatic tissue of control and *tert*-butyl hydroperoxide and cadmium chloride-treated rats by activating ERK1/2 signaling, which causes direct phosphorylation of Nrf2 at its serine 40 residues to stimulate its dissociation from keap1 (Park et al.,2016). On the other hand, another investigation has shown that ISL might stimulate the dissociation and nuclear translocation of Nrf2 by inducing an alkylation of Keap-1 at cysteine 151 rather than affecting Keap-1 expression (Luo et al., 2007). Therefore, further studies such as examining the inhibition of the Nrf2-keap1 interaction by the fluorescence polarization assay and molecular docking are highly encouraged. Unfortunately, these techniques are not yet established in our laboratory or institution and may be considered in future studies. In addition, these findings are still observational and need further support. Importantly, it could be better to repeat these experiments in animals or mesangial cells deficient in Nrf2 to confirm our data which should be considered in future studies.

In conclusion, our findings are novel to show a potent protective effect of ISL against DOX-mediated nephropathy in rats and indicate the role of the Nrf2/antioxidant axis in this protection. Given the high safety of ISL, these data might encourage to go further for more pre-clinical and clinical studies in cancer patients and investigate this protective effect. If proven to be effective, then ISL may provide a novel therapy that re-widen the clinical application of DOX in those patients.

Declaration of Competing Interest

The authors declare that they have no known competing financial interests or personal relationships that could have appeared to influence the work reported in this paper.

Acknowledgement

The authors extend their appreciation to the Deanship of Scientific Research at King Saud University for funding this work through research group No (RG- 1441-407).

Disclosure of Funding

This work was supported by the Deanship of Scientific Research at King Saud University (grant no RG- 1441-407).

References

Alzahrani, S., Said, E., Ajwah, S.M., Alsharif, S.Y., El-Bayoumi, K.S., Zaitone, S.A., Qushawy, M., Elsherbiny, N.M., 2021. Isoliquiritigenin attenuates inflammation and modulates Nrf2/caspase-3 signalling in STZ-induced aortic injury. J. Pharm. Pharmacol. 73 (2), 193–205.

Asaad, G.F., Hassan, A., Mostafa, R.E., 2021. Antioxidant impact of Lisinopril and Enalapril against acute kidney injury induced by doxorubicin in male Wistar rats: involvement of kidney injury molecule-1. Heliyon. 7 (1).

Bazzano, T., Restel, T.I., Porfirio, L.C., Souza, A.S., Silva, I.S., 2015. Renal biomarkers of male and female Wistar rats (Rattus norvegicus) undergoing renal ischemia and reperfusion. Acta. Cir. Bras. 30 (4), 277–288.

Biondo, L.A., Lima Junior, E.A., Souza, C.O., Cruz, M.M., Cunha, R.D.C., Alonso-Vale, M. I., Oyama, L.M., Nascimento, C.M.O., Pimentel, G.D., dos Santos, R.V.T., Lira, F.S., Rosa Neto, J.C., Peterson, J., 2016. Impact of doxorubicin treatment on the physiological functions of white adipose tissue. PLoS ONE 11 (3).

Canepari, M., Cappelli, V., Monti, E., Paracchini, L., Reggiani, C., 1994. Delayed doxorubicin cardiomyopathy in the rat: possible role of reduced food intake. Cardioscience. 5 (2), 101–106.

Cao, L.J., Li, H.D., Yan, M., Li, Z.H., Gong, H., Jiang, P., Deng, Y., Fang, P.F., Zhang, B.K., 2016. The protective effects of isoliquiritigenin and glycyrrhetinic acid against triptolide-induced oxidative stress in HepG2 cells involve Nrf2 activation. Evidence-based complementary and alternative medicine. eCAM 2016, 8912184.

Chen, X., Cai, X., Le, R., Zhang, M., Gu, X., Shen, F., Hong, G., Chen, Z., 2018. Isoliquiritigenin protects against sepsis-induced lung and liver injury by reducing inflammatory responses. Biochem. Biophys. Res. Commun. 496 (2), 245–252.

Elsherbiny, N.M., El-Sherbiny, M., 2014. Thymoquinone attenuates Doxorubicin-induced nephrotoxicity in rats: Role of Nrf2 and NOX4. Chem. Biol. Interact. 223, 102–108.

Ganesh Yerra, V., Negi, G., Sharma, S.S., Kumar, A., 2013. Potential therapeutic effects of the simultaneous targeting of the Nrf2 and NF-κB pathways in diabetic neuropathy. Redox Biol. 1 (1), 394–397.

Gao, Y., Lv, X., Yang, H., Peng, L., Ci, X., 2020. Isoliquiritigenin exerts antioxidative and anti-inflammatory effects via activating the KEAP-1/Nrf2 pathway and inhibiting the NF-κB and NLRP3 pathways in carrageenan-induced pleurisy. Food Funct. 11 (3), 2522–2534.

Guerrero-Hue, M., Rayego-Mateos, S., Vázquez-Carballo, C., Palomino-Antolín, A., García-Caballero, C., Opazo-Rios, L., Morgado-Pascual, J.L., Herencia, C., Mas, S., Ortiz, A., Rubio-Navarro, A., Egea, J., Villalba, J.M., Egido, J., Moreno, J.A., 2020. Protective role of Nrf2 in renal disease. Antioxidants (Basel). 10 (1), 39.

Guo, Z., Yan, M., Chen, L., Fang, P., Li, Z., Wan, Z., Cao, S., Hou, Z., Wei, S., Li, W., Zhang, B., 2018. Nrf2-dependent antioxidant response mediated the protective effect of tanshinone IIA on doxorubicin-induced cardiotoxicity. Exp. Ther. Med. 16 (4), 3333–3344.

Hennig, P., Garstkiewicz, M., Grossi, S., Di Filippo, M., French, L.E., Beer, H.D., 2018. The crosstalk between Nrf2 and inflammasomes. Int. J. Mol. Sci. 19 (2), 562.

Huang, X., Shi, Y., Chen, H., Le, R., Gong, X., Xu, K., Zhu, Q., Shen, F., Chen, Z., Gu, X., Chen, X., Chen, X., 2020. Isoliquiritigenin prevents hyperglycemia-induced renal injuries by inhibiting inflammation and oxidative stress via SIRT1-dependent mechanism. Cell Death Dis. 11 (12), 1040.

Huang, Z., Sheng, Y., Chen, M., Hao, Z., Hu, F., Ji, L., 2018. Liquiritigenin and liquiritin alleviated MCT-induced HSOS by activating Nrf2 antioxidative defense system. Toxicol. Appl. Pharmacol. 355, 18–27.

HWANG, Cheol, CHUN, Hong, 2012. Isoliquiritigenin Isolated from Licorice Glycyrrhiza uralensis Prevents 6-Hydroxydopamine-Induced Apoptosis in Dopaminergic Neurons. Bioscience, Biotechnology, and Biochemistry 76 (3), 536–543.

Lahoti, T.S., Patel, D., Thekkemadom, V., Beckett, R., Ray, S.D., 2012. Doxorubicin-induced in vivo nephrotoxicity involves oxidative stress-mediated multiple pro- and anti-apoptotic signaling pathways. Curr. Neurovasc. Res. 9 (4), 282–295.

Lee, C.K., Son, S.H., Park, K.K., Park, J.H., Lim, S.S., Chung, W.Y., 2008. Isoliquiritigenin inhibits tumor growth and protects the kidney and liver against chemotherapy-induced toxicity in a mouse xenograft model of colon carcinoma. J. Pharmacol. Sci. 106 (3), 444–451.

Liao, Y., Tan, R.Z., Li, J.C., Liu, T.T., Zhong, X., Yan, Y., Yang, J.K., Lin, X., Fan, J.M., Wang, L., 2020. Isoliquiritigenin Attenuates UUO-Induced Renal Inflammation and Fibrosis by Inhibiting Mincle/Syk/NF-Kappa B Signaling Pathway. Drug Des. Devel. Ther. 14, 1455–1468.

Lin, E.Y., Bayarsengee, U., Wang, C.C., Chiang, Y.H., Cheng, C.W., 2018. The natural compound 2,3,5,4'-tetrahydroxystilbene-2-O-β-d glucoside protects against adriamycin-induced nephropathy through activating the Nrf2-Keap1 antioxidant pathway. Environ. Toxicol. 33 (1), 72–82.

Liu, Q., Lv, H., Wen, Z., Ci, X., Peng, L., 2017. Isoliquiritigenin activates nuclear factor erythroid-2 related factor 2 to suppress the NOD-like receptor protein 3 inflammasome and inhibits the NF-κB pathway in macrophages and in acute lung injury. Front. Immunol. 8, 1518.

Luo, Y., Eggler, A.L., Liu, D., Liu, G., Mesecar, A.D., van Breemen, R.B., 2007. Sites of alkylation of human Keap1 by natural chemoprevention agents. J. Am. Soc. Mass Spectrom. 18 (12), 2226–2232.

Montorfano, I., Becerra, A., Cerro, R., Echeverría, C., Sáez, E., Morales, M.G., Fernández, R., Cabello-Verrugio, C., Simon, F., 2014. Oxidative stress mediates the conversion of endothelial cells into myofibroblasts via a TGF-β1 and TGF-β2-dependent pathway. Lab. Invest. 94 (10), 1068–1082.

Montoya, J.E., Luna, H.G., Morelos, A.B., Catedral, M.M., Lava, A.L., Amparo, J.R., Cristal-Luna, G.R., 2013. Association of creatinine clearance with neutropenia in breast cancer patients undergoing chemotherapy with fluorouracil, doxorubicin, and cyclophosphamide (FAC). Med. J. Malaysia 68 (2), 153–156.

Nordgren, K., Wallace, K.B., 2020. Disruption of the Keap1/Nrf2-antioxidant response system after chronic doxorubicin exposure in vivo. Cardiovasc. Toxicol. 20 (6), 557–570.

Olayanju, A., Copple, I.M., Bryan, H.K., Edge, G.T., Sison, R.L., Wong, M.W., Lai, Z.Q., Lin, Z.X., Dunn, K., Sanderson, C.M., Alghanem, A.F., Cross, M.J., Ellis, E.C., Ingelman-Sundberg, M., Malik, H.Z., Kitteringham, N.R., Goldring, C.E., Park, B.K., 2015. Brusatol provokes a rapid and transient inhibition of Nrf2 signaling and sensitizes mammalian cells to chemical toxicity-implications for therapeutic targeting of Nrf2. Free Radic. Biol. Med. 78, 202–212.

Owumi, S.E., Lewu, D.O., Arunsi, U.O., Oyelere, A.K., 2021. Luteolin attenuates doxorubicin-induced derangements of liver and kidney by reducing oxidative and inflammatory stress to suppress apoptosis. Hum. Exp. Toxicol. 40 (10), 1656–1672.

Park, S.M., Lee, J.R., Ku, S.K., Cho, I.J., Byun, S.H., Kim, S.C., Park, S.J., Kim, Y.W., 2016. Isoliquiritigenin in licorice functions as a hepatic protectant by induction of antioxidant genes through extracellular signal-regulated kinase-mediated NF-E2-related factor-2 signaling pathway. Eur. J. Nutr. 55 (8), 2431–2444.

Peng, F., Du, Q., Peng, C., Wang, N., Tang, H., Xie, X., Shen, J., Chen, J., 2015. A Review: The Pharmacology of Isoliquiritigenin. Phytother. Res. 29 (7), 969–977.

Ren, X., Bo, Y., Fan, J., Chen, M., Xu, D., Dong, Y., He, H., Ren, X., Qu, R., Jin, Y., Zhao, W., Xu, C., 2016. Dalbergioidin Ameliorates Doxorubicin-Induced Renal Fibrosis by Suppressing the TGF-β Signal Pathway. Mediators Inflamm. 2016, 5147571.

Sanz, A.B., Sanchez-Niño, M.D., Ramos, A.M., Moreno, J.A., Santamaria, B., Ruiz-Ortega, M., Egido, J., Ortiz, A., 2010. NF-kappaB in renal inflammation. J. Am. Soc. Nephrol. 21 (8), 1254–1262.

Savani, M., Woerner, K., Bu, L., Birkenbach, M., Skubitz, K.M., 2021. Pegylated liposomal doxorubicin-induced renal toxicity in retroperitoneal liposarcoma: a case report and literature review. Cancer Chemother. Pharmacol. 87 (2), 289–294.

Serafini, M.M., Catanzaro, M., Fagiani, F., Simoni, E., Caporaso, R., Dacrema, M., Romanoni, I., Govoni, S., Racchi, M., Daglia, M., Rosini, M., Lanni, C., 2020. Modulation of Keap1/Nrf2/ARE signaling pathway by curcuma- and garlic-derived hybrids. Front. Pharmacol. 10, 1597.

Shatoor, A.S., Al Humayed, S., Almohiy, H.M., 2022. Astaxanthin attenuates hepatic steatosis in high-fat diet-fed rats by suppressing microRNA-21 via transactivation of nuclear factor erythroid 2-related factor 2. J. Physiol. Biochem. 78 (1), 151–168.

Soltani Hekmat, A., Chenari, A., Alipanah, H., Javanmardi, K., 2021. Protective effect of alamandine on doxorubicin–induced nephrotoxicity in rats. BMC Pharmacol. Toxicol. 22 (1), 31.

Song, S., Chu, L., Liang, H., Chen, J., Liang, J., Huang, Z., Zhang, B., Chen, X., 2019. Protective effects of dioscin against doxorubicin-induced hepatotoxicity via regulation of Sirt1/FOXO1/NF-κb signal. Front. Pharmacol. 10, 1030.

Sullivan, D.E., Ferris, M., Nguyen, H., Abboud, E., Brody, A.R., 2009. TNF-alpha induces TGF-beta1 expression in lung fibroblasts at the transcriptional level via AP-1 activation. J. Cell Mol. Med. 13 (8B), 1866–1876.

Sun, L., Yang, Z., Zhang, J., Wang, J., 2021. Isoliquiritigenin attenuates acute renal injury through suppressing oxidative stress, fibrosis and JAK2/STAT3 pathway in streptozotocin-induced diabetic rats. Bioengineered. 12 (2), 11188–11200.

Sun, X., Li, X., Jia, H., Wang, H., Shui, G., Qin, Y., Shu, X., Wang, Y., Dong, J., Liu, G., Li, X., 2020. Nuclear factor E2-related factor 2 mediates oxidative stress-induced lipid accumulation in adipocytes by increasing adipogenesis and decreasing lipolysis. Antioxid. Redox Signal. 32 (3), 173–192.

Thorn, C.F., Oshiro, C., Marsh, S., Hernandez-Boussard, T., McLeod, H., Klein, T.E., Altman, R.B., 2011. Doxorubicin pathways: pharmacodynamics and adverse effects. Pharmacogenet. Genom. 21 (7), 440–446.

Wang, R., Zhang, C.Y., Bai, L.P., Pan, H.D., Shu, L.M., Kong, A.N., Leung, E.L., Liu, L., Li, T., 2015. Flavonoids derived from liquorice suppress murine macrophage activation by up-regulating heme oxygenase-1 independent of Nrf2 activation. Int. Immunopharmacol. 28 (2), 917–924.

Wardyn, J.D., Ponsford, A.H., Sanderson, C.M., 2015. Dissecting molecular cross-talk between Nrf2 and NF-κB response pathways. Biochem. Soc. Trans. 43 (4), 621–626.

Wu, X.Y., Luo, A.Y., Zhou, Y.R., Ren, J.H., 2014. N-acetylcysteine reduces oxidative stress, nuclear factor–κB activity and cardiomyocyte apoptosis in heart failure. Mol. Med. Rep. 10 (2), 615–624.

Xiong, D., Hu, W., Ye, S.T., Tan, Y.S., 2018. Isoliquiritigenin alleviated the Ang II-induced hypertensive renal injury through suppressing inflammation cytokines and oxidative stress-induced apoptosis via Nrf2 and NF-κB pathways. Biochem. Biophys. Res. Commun. 506 (1), 161–168.

Zhang, M., Wu, Y.Q., Xie, L., Wu, J., Xu, K., Xiao, J., Chen, D.Q., 2018. Isoliquiritigenin protects against pancreatic injury and intestinal dysfunction after severe acute pancreatitis via Nrf2 signaling. Front. Pharmacol. 9, 936.

Zhang, Y., Xu, Y., Qi, Y., Xu, L., Yin, L., Tao, X., Zhen, Y., Han, X., Song, S., Ma, X., 2019. Corrigendum to“ Protective effects of dioscin agains doxorubicin-induced nephrotoxicity via adjusting FXR-mediated oxidative stress and inflammation”[Toxicology 378 (2017) 53–64]. Toxicology 424, 152251.

Zhao, Y., Ding, W.X., Qian, T., Watkins, S., Lemasters, J.J., Yin, X.M., 2003. Bid activates multiple mitochondrial apoptotic mechanisms in primary hepatocytes after death receptor engagement. Gastroenterology 125 (3), 854–867.

Zhao, Z., Park, S.M., Guan, L., Wu, Y., Lee, J.R., Kim, S.C., Kim, Y.W., Zhao, R., 2015. Isoliquiritigenin attenuates oxidative hepatic damage induced by carbon tetrachloride with or without buthionine sulfoximine. Chem. Biol. Interact. 225, 13–20.